

V-Reactor Dynamics: Dual Chaotic Systems and Synchronizing Human Defenses with Viral Evolution

Yong-Shou Chen

China Institute of Atomic Energy, Beijing 102413, China

The COVID-19 pandemic exposed critical gaps in our ability to predict viral emergence and trajectory. Moving beyond sequence-dependent surveillance, we introduce V-Reactor Dynamics, a physics-based framework that models host-virus interaction as a synchronized dual chaotic system. At its core is the reactivity parameter (ρ), a measurable quantity derived from viral replication, immune neutralization, and drug interaction cross sections. We show that ρ dictates both intra-host viral load phases, peak ($\rho > 0$), plateau ($\rho \approx 0$), and clearance ($\rho < 0$), and, through a scaling law, the Lyapunov Exponent governing population-level transmission dynamics. Retrospectively, the model correctly differentiates SARS-CoV-2's higher transmissibility from SARS-CoV's lethality, accurately forecasts Omicron waves, and quantifies trade-offs between lockdown intensity and socioeconomic cost. Crucially, V-Dynamics enables pre-outbreak prediction via in vitro measurement of viral reaction cross sections, offering a pathway to proactive pandemic defense. By integrating quantum-mechanical interaction models with chaos theory across scales, this framework provides a quantitative roadmap for anticipating, controlling, and ultimately preempting future viral threats.

The persistent threat of viral pandemics, exemplified by the devastating global impact of COVID-19, underscores a fundamental scientific and public health challenge: our inability to predict the emergence, transmission, and virulence of novel viruses. Despite advances in genomic sequencing and molecular virology, the reactive, sequence-dependent paradigm remains inadequate for forecasting viral behavior before widespread outbreaks occur. This limitation was starkly revealed during the SARS-CoV-2 pandemic, where high transmissibility and immune evasion emerged unexpectedly, leading to unprecedented morbidity, mortality, and socioeconomic disruption. Current predictive models, largely based on epidemiological fitting or phylogenetic extrapolation, lack a mechanistic, physics-based foundation capable of integrating viral replication dynamics, host immune response, and population-scale transmission into a unified predictive framework. To address this gap, we introduce V-Reactor Dynamics (V-Dynamics), a novel interdisciplinary framework that conceptualizes host-virus interactions as a synchronized dual chaotic system, inspired by reactor physics and chaos theory. At its core, V-Dynamics quantifies viral dynamics through the reactivity parameter (ρ), a physically measurable quantity derived from virion-host interaction cross sections. We demonstrate that ρ not only governs intra-host infection phases—peak ($\rho > 0$), plateau ($\rho \approx 0$),

and clearance ($\rho < 0$)—but also, through a scaling law, determines the Lyapunov Exponent of population-level transmission chaos. This enables a predictive link between microscopic viral replication efficiency and macroscopic pandemic trajectory. Here, we present the theoretical foundation of V-Dynamics, derive its governing equations, and validate its predictive power through retrospective analyses of SARS-CoV, SARS-CoV-2, and Omicron variant outbreaks. We further propose a pathway toward pre-outbreak prediction via in vitro measurement of viral reaction cross sections, offering a transformative shift from descriptive to predictive virology. By bridging quantum mechanics, kinetic theory, and nonlinear dynamics, this framework provides a quantitative, actionable roadmap for anticipating and mitigating future viral threats.

Concepts of V-reactor dynamics

The virus(V)-reactor dynamics is introduced from a physics perspective to explain SARS-CoV-2 infection in human lungs and its pandemic spread. The key concepts are presented as follows.

Virion replication reaction. A virion replication reaction is a viral process in which a host cell (H-particle) is bombarded by a virion, undergoes transformation into a destroyed H-particle, and releases new virions. These released virions can then infect other H-particles, creating a chain reaction that may be controlled within a diseased lung core or become uncontrolled, leading to severe outcomes.

Self-sustaining virion chain reaction. This is a viral replication process in which virions released from one H-particle infect and destroy other H-particles, releasing more virions in a continuous, self-amplifying cascade. The reaction becomes self-sustaining when, on average, each replication event produces enough virions to trigger at least one more replication event. In a V-reactor, this chain reaction is often controlled through immune responses, where antibodies (A-particles) neutralize virions, establishing a transient balance between virion production and destruction.

V-reactor hypothesis. We hypothesize that a virus-infected human lung can be modeled as a virion V-reactor analogous to a neutron reactor, based on a physics-driven perspective. The central concept is the self-sustaining virion chain reaction. This can be summarized as: a V-reactor is an assembly of human lung material capable of sustaining and controlling a virion chain reaction with H-particles as fuel. Experimental studies using inoculated human lung tissue explants with SARS-CoV-2 or SARS-CoV have observed such self-sustaining reactions, with virion counts increasing a hundredfold within 2 to 48 hours for SARS-CoV-2^[1].

Core equations in V-reactor dynamics

The fundamental equations of V-reactor dynamics are derived from a diffusion equation describing virion motion through the reactor core, including scattering, absorption, and leakage (see Methods).

Viral kinetic equation. Under assumptions leading to the point reactor model, the viral kinetic equation is derived as:

$$\frac{dn_V(t)}{dt} = \frac{\rho}{\ell} n_V(t), \quad (1)$$

where $n_V(t)$ is the virion density, ρ is reactivity, and ℓ is generation time, expressed as:

$$\rho = \frac{k_{eff} - 1}{k_{eff}}, \ell = \frac{\ell_0}{k_{eff}}. \quad (2)$$

Here, k_{eff} is the effective multiplication constant (ratio of virions produced to those lost), and ℓ_0 is the virion effective lifetime. Given initial conditions $n_V^0 = n_V(t=0)$ and time-dependent $\rho(t)$, the solution is:

$$n_V(t) = n_V^0 \exp\left(\frac{1}{\ell} \int_0^t \rho(t) dt\right). \quad (3)$$

For a basic reactivity mode $\rho(t) = \rho_0 - \gamma t$, where $\rho_0 \geq 0$ and $\gamma \geq 0$, the solution becomes:

$$n_V(t) = n_V^0 \exp\left(\frac{\rho_0}{\ell} t - \frac{\gamma}{2\ell} t^2\right). \quad (4)$$

Expressions of Reactivity and Generation time. Reactivity ρ and generation time ℓ defined in Eq.(2) are related to virion interaction constants - cross sections, and ρ/ℓ can be expressed as:

$$\rho/\ell = v(\nu\sigma_r N_H - \sigma_a N_A - \sigma_a^D N_D - DB^2). \quad (5)$$

Where σ_r , σ_a and σ_a^D are cross sections for replication with host cells, neutralization with antibodies, and absorption with drug particles, respectively. ν is the average number of virions produced per replication event, v is the velocity of virions. N_H , N_A , and N_D are the densities for host cells, antibodies, and drugs, respectively. This enables to predict quantitatively the dynamic balances between viral replication, immune response, drug efficacy, and virion loss via leakage during infection.

Burnup equation of H-particles. This equation describes the decline in H-particle concentration due to viral replication, with cellular burnout severity linked to clinical mortality. Neglecting feedback effects, it is written as:

$$\frac{dN_H(t)}{dt} = -\sigma_a \phi N_H(t), \quad (6)$$

where N_H is H-particle density, $\sigma_a = \sigma_c + \sigma_r$ is the virion absorption cross section, and $\phi = \nu n_V$ is the virion flux in the lung core. Fuel consumption is defined as N_H/N_H^0 , and $N_H^0 = N_H(t=0)$.

Equation of viral production chaos. The chaotic dynamics of viral production, represented by the viral load $n_V(t)$, is modeled by

$$n_V(h) = \frac{n_0 n_\infty}{n_0 + n_\infty \exp(-\lambda_V h)}. \quad (7)$$

Where $\lambda_V = \rho_0/\ell$ is the Lyapunov Exponent (LE), h (in hours) represents the time from the start of the epidemic, $n_0 = n_V(t=0)$, and $n_\infty = n_V(t \rightarrow \infty)$ is a finite saturation value.

Equation of viral spread. Equation of viral spread. Integrating viral dynamics with chaos theory yields a population-level transmission equation for the number of positive cases N_{pos} :

$$N_{pos}(d) = \frac{N_0 N_\infty}{N_0 + N_\infty \exp(-\lambda d)}. \quad (8)$$

Where λ is the Lyapunov Exponent, d (in days) represents the time from the start of the epidemic, $N_0 = N_{pos}(t=0)$, and $N_\infty = N_{pos}(t \rightarrow \infty)$ is a finite saturation value. The two LEs satisfy the scaling law: $\lambda = \chi \lambda_V$, where $\chi \sim 10^{-2}$ is a dimensionless scaling exponent determined from empirical data.

Dual Chaotic Systems and the Rate Scaling Law

In the 1990s, the emerging field of chaos theory proposed that diverse complex systems could share underlying commonalities, often describable through simple mathematical maps. A central concept in this framework is the Lyapunov Exponent (LE), which quantifies the rate of separation between initially proximate system trajectories over time. We propose that transmissible viruses operate within two intrinsically linked chaotic systems: the intra-host viral production system (within an infected individual) and the inter-host transmission system (within a population). We have formalized this dual-chaotic framework, deriving its governing equations (Eqs.7, 8) and establishing a constitutive connection through an LE scaling law. Existing chaos-theoretic models of SARS-CoV-2 transmission are largely descriptive, treating the LE as a free fitting parameter, which inherently limits their predictive power^[2]. Our model advances beyond this by deriving the population-level LE from first principles, removing its status as a mere adjustable parameter. In the absence of an effective immune response or clinical intervention, the intra-host system, driven by a constant positive reactivity (Fig.1d), can enter a runaway chaotic state, culminating in an extremely high viral load saturation associated with patient death (Fig.1c). For instance, a sputum sample from a fatal case on day 8 post-onset contained 1.34×10^{11} copies/ml^[3], whereas peak loads in non-fatal cases, typically observed around day 3 post-onset, are usually on the order of $\sim 1 \times 10^6$ copies/mL (Fig.1a). In most non-fatal infections, viral loads deviate from pronounced chaotic growth, peaking around 3 days post-onset before declining sharply as the adaptive immune response activates, driving reactivity from positive to negative (Fig.1b). The critical window for preventing progression to a dangerous, high-chaos state is thus the first few days post-onset, prior to the system entering uncontrolled exponential growth. Optimized antiviral strategies can be designed to drive the intra-host Lyapunov Exponent λ_V toward negative values, which would subsequently induce a synchronized reversal in the population transmission dynamics. The sign reversal of both Lyapunov Exponents would, within this framework, mark the end of a viral pandemic.

Viral dynamics of SARS-CoV-2

Using the viral kinetic equation, we quantitatively describe SARS-CoV-2 dynamics by analyzing virion interactions with H-particles (replication) and A-particles (immune response). Data from patients in Germany^[4] and China^[3] were used for validation.

Viral load dynamics and phases. Viral load dynamics are modeled with a stepwise reactivity pattern and each step having a mode of $\rho(t) = \rho_0 - \gamma t$. Equation (4) gives the viral load $n_V(t)$. Our analysis identifies distinct infection phases driven by immune response shifts. Modeled viral loads align with experimental data from the upper respiratory tract, capturing peak, plateau, and clearance phases (Fig. 1a). Current studies of viral dynamics often rely on mathematical models fitted to data^[5]. Unlike phenomenological models, our framework provides a first-principles predictive approach.

Origin of viral load phase transition. Phase transitions are driven by reactivity switching (Fig. 1b). The peak phase ($\rho > 0$) corresponds to viral growth, the plateau phase ($\rho \approx 0$) to quasi-equilibrium, and the clearance phase ($\rho < 0$) to immune domi-

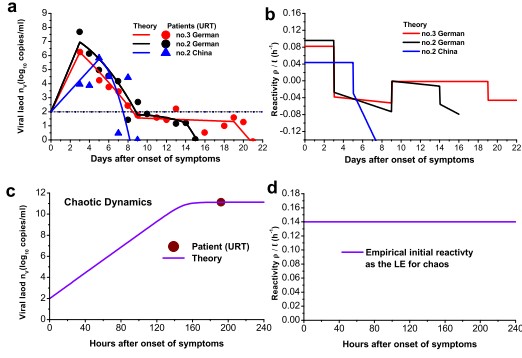


Figure 1: Viral load dynamics of SARS-CoV-2 predicted by V-Dynamics. **a** Theoretical viral load curves (solid lines) compared to upper respiratory tract (URT) data from patients in China (No. 2)^[3] and Germany (No. 2 and 3)^[4]. Dashed blue line indicates detection limit. **b** Corresponding reactivity ρ/l (h^{-1}) driving the viral load phases: peak ($\rho > 0$), plateau ($\rho \approx 0$), and clearance ($\rho < 0$). **c** The chaotic viral load simulated using Eq. (7) with $\lambda_V = 014h^{-1}$, typical initial ρ_0/l (Fig. 2c), compared to upper respiratory tract (URT) data from patient who died^[3]. **d** Corresponding reactivity ($\rho > 0$ over time) driving the chaotic dynamics.

nance. Reactivity shifts are triggered by immune response changes or drug interventions.

V-dynamics predictive capacity and accuracy

V-dynamics predicts virus transmission speed, pathogenicity, and impacts on public health, society, and economy. Its accuracy stems from modeling viral dynamics as a dual chaotic system, where Lyapunov Exponents (LE) are governed by ρ/l .

Prediction at the early stage of outbreak. Early viral load data are used to extract ρ/l , enabling estimation of transmission rate and virulence. Retrospective simulations for SARS-CoV-2 and SARS-CoV show distinct reactivity patterns and transmission speeds (Fig. 2). SARS-CoV-2 exhibits higher initial reactivity and faster spread.

Viral transmission speed. Using Eq.(8) with $N_0 = 10$ and $N_\infty = 18,910.0$, and $\lambda = 0.05\rho_0/l$, SARS-CoV-2 reaches saturation about three times faster than SARS-CoV (Fig. 3c).

Host Cell Consumption (Burnup). Simulated lung-core viral loads (scaled down by 1/500 from URT data) and theoretical cross section $\sigma_a = 2.775 \times 10^{-11} cm^2$ were used in Eq.(6) to compute H-particle burnup (Fig. 3b). SARS-CoV causes greater cell damage, correlating with higher lethality. Indeed, in the two outbreaks, SARS-CoV-2 has proven to be more transmissible and to have a lower death rate than SARS-CoV^[7, 8].

Real time clinical treatment. Reactivity monitoring enables phase-specific interventions, especially during the peak phase. We propose an AI-driven Reactivity Tracker (AI-RT) for real-time, personalized treatment adjustment.

Pre-outbreak prediction. Pre-outbreak forecasting uses in vitro viral reaction cross section (σ) data to compute ρ and l , enabling transmission and virulence predictions. This represents a shift from descriptive to predictive virology.

Forecasting prediction of impacts of local outbreaks. Early reactivity data allow estimation of local outbreak progression. We

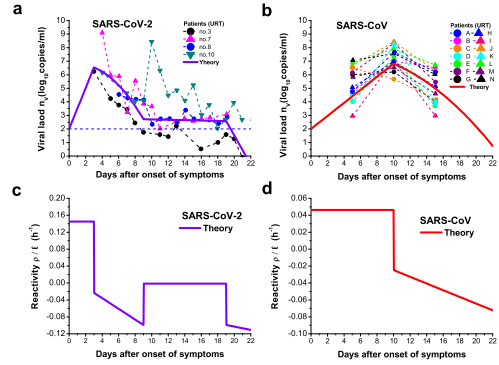


Figure 2: Comparative viral kinetics of SARS-CoV-2 and SARS-CoV. **a** Modeled SARS-CoV-2 viral load (violet) versus URT data from four German patients^[4]. Detection limit shown as dashed line. **b** Modeled SARS-CoV viral load (red) versus data from 14 Chinese patients^[6]. **(c, d)** Reactivity ρ/l (h^{-1}) used to generate curves in **a** and **b**, respectively. SARS-CoV-2 exhibits a multi-step reactivity pattern and higher initial ρ/l , correlating with enhanced transmissibility.

fitted the Eq.(8) parameters to Omicron infection data from Hong Kong and Shanghai^[9]. Simulations for Omicron outbreaks in both cities (Fig. 4) show how intervention policies affect saturation infection levels, highlighting trade-offs between infection control and socioeconomic costs.

In vitro measurement of virus-cell interactions

V-reactor dynamics defines virus-cell interaction constants and proposes their quantification via in vitro experiments. We aim to measure cross sections for replication (σ_r), antibody neutralization (σ_a), and drug action (σ_d). Advanced biophysical techniques and AI-driven systems will be employed to observe single replication events, providing a foundation for predictive virology and antiviral design. The existing in vitro measurement monitors viral load growth in inoculated tissue with SARS-CoV-2, capturing net replication dynamics, but they do not isolate the underlying interaction constant^[1].

Conclusion

In summary, V-Reactor Dynamics establishes a physics-based, predictive framework for virology by modeling host-virus interaction as a dual chaotic system governed by the reactivity parameter ρ . We have shown that ρ integrates microscopic viral replication, immune neutralization, and drug interaction into a single quantifiable metric that dictates both intra-host infection phases and population-level transmission dynamics. Through a scaling law linking viral production chaos to transmission chaos, V-Dynamics provides a mechanistic basis for forecasting pandemic trajectories from early viral load data or even pre-outbreak in vitro measurements. Retrospective validation with SARS-CoV, SARS-CoV-2, and Omicron outbreaks confirms the model's capacity to differentiate transmission speed from lethality, predict wave progression, and evaluate intervention trade-offs. Crucially, the framework enables pre-outbreak risk assessment through experimental measurement of viral reaction cross sections, a move toward proactive rather than reactive pandemic preparedness. Looking forward, V-Dynamics opens several translational pathways: the de-

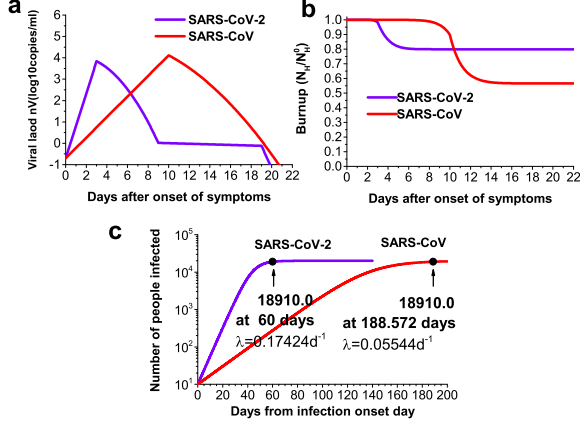


Figure 3: Simulated host cell damage and population transmission dynamics. **a** Estimated viral loads in lung core for SARS-CoV-2 (violet) and SARS-CoV (red). **b** Corresponding H-particle burnup (host cell depletion) derived from Eq.(6). SARS-CoV induces greater cell damage, aligning with higher lethality. **c** Cumulative infections over time predicted by Eq.(8) using Lyapunov Exponents scaled from initial reactivity rates. SARS-CoV-2 reaches saturation ~ 3 times faster than SARS-CoV, reflecting its higher transmissibility.

velopment of an AI-driven reactivity tracker (AI-RT) for real-time clinical monitoring, the design of broad-spectrum antivirals based on optimized cross sections, and the integration of functional interaction data into global surveillance systems. While challenges remain in high-precision cross-section measurement and model refinement through interdisciplinary collaboration, this paradigm shift toward predictive virology promises to synchronize human defense mechanisms with viral evolution. Ultimately, V-Dynamics redefines our approach to pandemic preparedness, offering a scientifically grounded, quantitatively predictive toolset for navigating future viral threats with greater foresight, precision, and resilience. Real-time monitoring of ρ via an AI-driven reactivity tracker could enable personalized treatment and early outbreak containment, paving the way for a new era of precision antiviral intervention.

Acknowledgements The author thanks Evelyn Jiang for valuable discussions on the SARS-CoV-2 pandemic. This work was supported by the Continuous Basic Scientific Research Project (WDJC-2019-13, BJ20002501) and the National Natural Science Foundation of China (11790325, 11975314).

Author contributions The author proposed, designed, and completed all aspects of this research.

Author Information The author declares no competing financial interests. Correspondence should be addressed to Y.-S. Chen (yshouchen@163.com).

Methods

Virion Diffusion Equation and Kinetic Derivation

We model the diffusion of virions within infected lung tissue analogously to neutron diffusion in a nuclear reactor. Starting from the Boltzmann transport equation and applying the isotropic and single-speed approximation, we derive the virion diffusion equa-

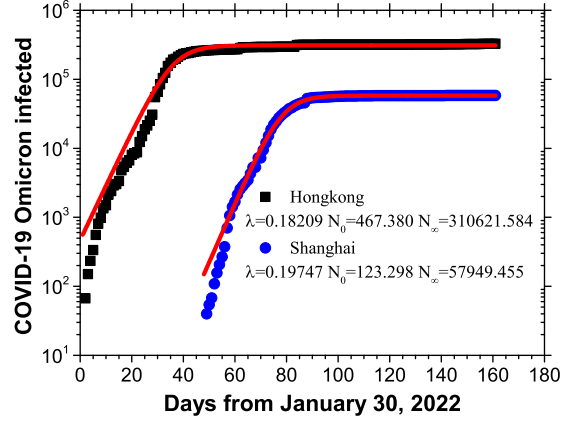


Figure 4: Retrospective prediction of Omicron outbreaks in Hong Kong and Shanghai. Modeled cumulative infections (curves) compared to reported case data (points). Fitted saturation levels (N_∞) reflect differential impacts of intervention policies: strict lockdowns in Shanghai reduced N_∞ by ~ 81 percent compared to Hong Kong, highlighting the trade-off between infection control and socioeconomic cost.

tion:

$$\frac{\partial n_v(\vec{r}, t)}{\partial t} = Dv\nabla^2 n_v(\vec{r}, t) - \Sigma_a v n_v(\vec{r}, t) + S(\vec{r}, t). \quad (9)$$

Where $n_v(\vec{r}, t)$ is the virion number density as a function of position \vec{r} and time t , D is the diffusion coefficient, v is the average virion velocity, Σ_a is the macroscopic absorption cross section, $S(\vec{r}, t)$ is the source term accounting for virion production and external input. The source term is expressed as:

$$S(\vec{r}, t) = k_\infty \Sigma_a v n_v(\vec{r}, t) + S_0(\vec{r}, t), \quad (10)$$

where k_∞ is the effective multiplication constant for an infinite medium, representing the average number of virions produced per absorption event.

Spatial Separation Assumption and Point Reactor Model

We assume separability of the virion density into spatial and temporal components:

$$n_v(\vec{r}, t) = f(\vec{r})n_v(t). \quad (11)$$

Substituting into the diffusion equation, the spatial component satisfies the Helmholtz equation:

$$\nabla^2 f(\vec{r}) + B^2 f(\vec{r}) = 0. \quad (12)$$

Where B^2 is the buckling factor, accounting for leakage losses. This leads to the virion kinetic equation:

$$\frac{dn_v(t)}{dt} = \frac{k_\infty - (1 + L^2 B^2)}{\ell_\infty} n_v(t) + q(t), \quad (13)$$

which corresponds to the point reactor model, applicable under uniform virion density assumptions in a homogeneous medium.

Definition and Expressions of Reactivity (ρ) and Generation Time (ℓ)

The reactivity ρ is equal to the ratio of the net growth in number of virions to the number of virions produced, and the generation time ℓ is inversely proportional to the virion production per second. The two key kinetic parameters are defined as:

$$\rho = \frac{k_{eff} - 1}{k_{eff}}, \quad \ell = \frac{\ell_0}{k_{eff}}. \quad (14)$$

Where $k_{eff} = k_{\infty}/(1 + L^2B^2)$ is the effective multiplication constant, $\ell_0 = \ell_{\infty}/(1 + L^2B^2)$ is the mean virion lifetime, $L^2 = D/\Sigma_a$ defines the diffusion length L , and $1/(1 + L^2B^2)$ represents the fraction of virions which escape leakage. These can also be expressed in terms of production and loss rates:

$$\rho = \frac{\nu\Sigma_r - (\Sigma_a + DB^2)}{\nu\Sigma_r}, \quad \ell = \frac{1}{\nu\Sigma_r}. \quad (15)$$

where ν is the average number of virions produced per replication event, and $\Sigma_r = \sigma_r N_H$ is the macroscopic replication cross section. $\nu\Sigma_r$ and νDB^2 denote the virion production rate and virions loss rate due to leakage, respectively. By substituting Eq.(14), Eq. (13) becomes:

$$\frac{dn_v(t)}{dt} = \frac{\rho}{\ell} n_v(t) + q(t). \quad (16)$$

Virion Interaction Cross Sections with Host Cells

Drawing an analogy to quantum scattering, we introduce microscopic cross sections to quantify the probability of interaction between virions and host cells, antibodies, or drug molecules. Key cross sections include: Replication cross section σ_r , probability of successful viral entry, replication, and release; Absorption cross section σ_a , probability of virion neutralization by antibodies or binding by drugs; Capture cross section σ_c , probability of virion capture without replication. These satisfy $\sigma_a = \sigma_r + \sigma_c$. In the initial model, we assume $\sigma_c \approx 0$, simplifying to $\sigma_r = \sigma_a$.

Host Cell Burnup Equation

Assuming host cells (H-particles) are consumed during viral replication or capture, and that this consumption does not significantly affect virion flux, we derive the burnup equation:

$$\frac{dN_H}{dt} = -\sigma_a \phi N_H. \quad (17)$$

Where N_H is the host cell number density, $\phi = \nu n_v$ is the virion flux. The solution is:

$$N_H(t) = N_H^0 \exp(-\sigma_a \nu \int_0^t n_v(t) dt). \quad (18)$$

Where the N_H^0 is the initial number density, ν is the velocity of virions.

Chaotic Models of Viral Production and Transmission

The viral load, $n_v(t)$, grows exponentially at a rate characterized by a positive initial reactivity, $n_v(t) = n_0 \exp((\rho_0/\ell)t)$, and can be interpreted as the chaotic divergence quantity. Within the framework of chaos theory^[10, 11], this defines microscopic viral production chaotic system that is modeled as:

$$n_v(t) = \frac{n_0 n_{\infty}}{n_0 + n_{\infty} \exp(-\lambda_v(t))}, \quad (19)$$

where $\lambda_v = \rho_0/\ell$ is the Lyapunov Exponent governing the chaotic growth, n_0 is initial perturbation and n_{∞} is final saturation. Similarly, we model viral spread within a population as a chaotic system, represented as number of people infected, N_{pos} , and is modeled as:

$$N_{pos}(t) = \frac{N_0 N_{\infty}}{N_0 + N_{\infty} \exp(-\lambda t)}, \quad (20)$$

which captures the saturation dynamics of an outbreak. We postulate a power-law relationship coupling the two systems, $N_{pos}(t) = n_v(t)^\chi$, which leads to the scaling law, $\lambda = \chi \lambda_v$, where $\chi \sim 10^{-2}$ is a dimensionless scaling exponent determined from empirical data.

Proposed Experimental Measurements: In Vitro Cross Section and Reactivity Determination

To enable pre-outbreak prediction, we propose in vitro measurement of virion interaction cross sections using an integrated experimental system combining: super-resolution microscopy, microfluidic platforms, single-virion tracking, and real-time data acquisition and AI-enhanced analysis. Measured cross sections ($\sigma_r, \sigma_a, \sigma_a^D$) allow computation of ρ and ℓ , enabling prediction of transmission rates and virulence based on first principles. This represents a shift from descriptive to predictive virology grounded in quantifiable biophysical constants. Using Eq.(15) and considering drug effect, the ρ/ℓ may be expressed as,

$$\rho/\ell = \nu(\sigma_r N_H - \sigma_a N_A - \sigma_a^D N_D - DB^2). \quad (21)$$

Where N_A is antibody density, N_D is drug particle density. Terms in the equation represent contributions respectively from virion production, immune response, drug efficacy, and leakage loss, which tells that mechanical ventilations should be used in patients with respiratory failure.

Calculation of Cross Section for Virus-cell Interactions

We present a method for computing cross sections applicable to reactions between biological particles. The microscopic cross section represents the probability of a specific interaction as a function of the incident particle's kinetic energy. From a quantum mechanical perspective, the cross section for an incident particle striking a target is given by $\pi(\lambda_d + R)^2$, where R is the target radius and λ_d is the de Broglie wavelength of the incident particle, expressed as $\lambda_d = h/\sqrt{2Em}$, and the Planck's constant, $h = 6.626 \times 10^{-27}$ erg sec. Using a virion mass of $m = 1.0 \times 10^{-15}$ g and a physiological temperature of $T = 39^\circ C$, λ_d is estimated to be $\sim 1.14 \times 10^{-13}$ cm, which is ~ 10 orders of magnitude smaller than the diameter of a host (H) cell. Thus, for thermal virions, the wave-like contribution to the cross section is negligible - unlike in nuclear collisions (e.g., neutron-nucleus interactions), where it may dominate. Moreover, the cross sections for virion replication or adsorption are not accurately described by the geometric area πR^2 of the host cell. We therefore introduce an effective cross-sectional area tailored to biological collisions. For SARS-CoV-2, cellular entry is mediated by binding of the viral spike glycoprotein to angiotensin-converting enzyme 2 (ACE2) receptors on the host cell surface^[12]. The key interface is the receptor-binding domain (RBD) of the spike protein. We define the effective cross-sectional area as the total target area presented by accessible ACE2 receptors to an approaching virion, approximated as the product of the RBD area and half the number of ACE2 receptors per cell. The RBD diameter is approximately 4.8 - 4.9 nm^[13], corresponding to an area of $1.85 \times 10^{-13} \text{ cm}^2$. The number of ACE2 receptors per cell varies widely across individuals, ranging from fewer than ten to several hundred^[14, 15]. Adopting an estimate of 300 ACE2 receptors per cell, the resulting adsorption cross section is $\sigma_a = 2.775 \times 10^{-11} \text{ cm}^2$, roughly four orders of magnitude smaller than the geometric cross section πR^2 . We note that σ_a represents the cross section for virus binding to the cell surface, not necessarily for successful internalization. While ACE2 is essential for SARS-CoV-2 entry^[16, 17], post-binding entry mechanisms and their quantitative effects on infection efficiency remain to be fully incorporated into this cross section model.

Overview of development potential of V-reactor dynamics

It should be noted that although V-reactor dynamics serves as a fundamental predictive virology paradigm, it holds the potential to address a variety of more complex issues. For instance, consider the scenario involving multiple types of target cells. Clinical stud-

ies on COVID-19 have revealed a significant reduction in lymphocyte counts among severe patients, as well as severe inflammatory responses that drive a large influx of lymphocytes into the lungs [18, 19]. This suggests that lymphocytes may act as target cells, with new target cells emerging over time. In practice, we can incorporate the effects of both increasing types and quantities of target cells into the equations. This approach is analogous to accounting for the generation of new fuel, such as Pu239, in nuclear reactor dynamics theory.

References

- [1] Hin. Chu, et al. Comparative Replication and Immune Activation Profiles of SARS-CoV-2 and SARS-CoV in Human Lungs: An Ex Vivo Study With Implications for the Pathogenesis of COVID-19. *CID* 71, 1400-1409 (2020).
- [2] Aldo Bonasera and Suyalatu Zhang, Chaos, Percolation and the Coronavirus Spread, *Frontiers in Physics*, Volume 8, article 171, 1-6 (2020).
- [3] Y. Pan, D. Zhang, P. Yang, L.L.M. Poon, Q. Wang, Viral load of SARS-CoV-2 in clinical samples, *Lancet Infect. Dis.* (2020) S1473-3099(20)30113-4. [http://dx.doi.org/10.1016/S1473-3099\(20\)30113-4](http://dx.doi.org/10.1016/S1473-3099(20)30113-4). PubMed PMID: 32105638.
- [4] R. Wolfel, VM. Corman, W. Guggemos, et al., Virological assessment of hospitalized patients with COVID-2019 *Nature* 581, 465-469 (2020) <http://dx.doi.org/10.1038/s41586-020-2196-x>.
- [5] Sunpeng Wang, Yang Pan, Quanyi Wang, Hongyu Miao, Ashley N. Brown, Libin Rong, Modeling the viral dynamics of SARS-CoV-2 infection *Mathematical Biosciences* 328 (2020) 108438 <https://doi.org/10.1016/j.mbs.2020.108438>
- [6] JS Peiris, CM Chu, VC Cheng, et al., Clinical progression and viral load in a community outbreak of coronavirus associated SARS pneumonia: a prospective study *Lancet* 361: 1767-72 (2003).
- [7] Michael A. Johansson, Talia M. Quandelacy, Sarah Kada, et al. SARS-CoV-2 Transmission From People Without COVID-19 Symptoms *JAMA Network Open*. 2021;4(1):e2035057. doi:10.1001/jamanetworkopen.2020.35057
- [8] Eskild Petersen, Marion Koopmans, Unyeong Go, et al. Comparing SARS-CoV-2 with SARS-CoV and influenza pandemics www.thelancet.com/infection Vol 20 August 2020, e238 - e244.
- [9] Hongkong and Shanghai coronavirus data 2022: https://wp.m.163.com/163/page/news/virus_report/index.html_nw=1&_anw=1, https://news.sina.cn/zt_d/yiqing0121
- [10] E. Ott *Chaos in dynamical systems*, Cambridge University Prtess, Englandf, 1993; Hilborn RC. *Chaos an nonlinear dynamics*, Oxford University Prtess, New York, 1994.
- [11] A. Bonasera, V. Latora and A. Rapisarda, *Phys. Rev. Lett.* (1995) 75, 3434.
- [12] Jun Lan, Jiwan Ge, Jinfang Yu, et al. Structure of the SARS-CoV-2 spike receptor-binding domain bound to the ACE2 receptor *Nature* 581, 215-220 (2020) doi.org/10.1038/s41586-020-2180-5
- [13] Cecylia S. Lupala , Yongjin Ye , Hong Chen , Xiao-Dong Su, Haiguang Liu. Mutations on RBD of SARS-CoV-2 Omicron variant result in stronger binding to human ACE2 receptor *Biochemical and Biophysical Research Communications* 590, 34e41 (2022). <https://doi.org/10.1016/j.bbrc.2021.12.079>
- [14] Hao Xu, Liang Zhong, Jiabin Deng, et al. High expression of ACE2 receptor of 2019-nCoV on the epithelial cells of oral mucosa *International Journal of Oral Science* (2020) 12:8 <https://doi.org/10.1038/s41368-020-0074-x>
- [15] Guoping Li, Xiang He, Lei Zhanga, et al. Assessing ACE2 expression patterns in lung tissues in the pathogenesis of COVID-19 *Journal of Autoimmunity* 112 (2020) 102463 <https://doi.org/10.1016/j.jaut.2020.102463>
- [16] A. C. Walls, et al. Structure, function, and antigenicity of the SARS-CoV-2 spike glycoprotein. *Cell* <https://doi.org/10.1016/j.cell.2020.02.058> (2020).
- [17] Hoffmann, M. et al. SARS-CoV-2 cell entry depends on ACE2 and TMPRSS2 and is blocked by a clinically proven protease inhibitor. *Cell* <https://doi.org/10.1016/j.cell.2020.02.052> (2020).
- [18] X. Wang, W. Xu, G. Hu, S. Xia, Z. Sun, Z. Liu, et al., SARS-CoV-2 infects T lymphocytes through its spike protein-mediated membrane fusion, *Cell. Mol. Immunol.* (2020) <http://dx.doi.org/10.1038/s41423-020-0424-9>.
- [19] Z. Xu, L. Shi, Y. Wang, J. Zhang, L. Huang, C. Zhang, et al., Pathological findings of COVID-19 associated with acute respiratory distress syndrome, *Lancet Respir. Med.* (2020) S2213-600(20)30076-X. [http://dx.doi.org/10.1016/S2213-2600\(20\)30076-X](http://dx.doi.org/10.1016/S2213-2600(20)30076-X). PubMed PMID: 32085846.